Nanoscale Thermal Imaging of VO$_2$ via Poole-Frenkel Conduction

Alyson Spitzig,[1, 2] Adam Pivonka,[1] Harry Mickalide,[1] Alex Frenzel,[1] Jeehoon Kim,[1] Changhyun Ko,[3] You Zhou,[4]
Kevin O'Connor,[1] Eric Hudson,[1] Shriram Ramanathan,[3] Jennifer E. Hoffman,[2, 1, *] and Jason Hoffman[1, 2, †]

[1]*Department of Physics, Harvard University, Cambridge, Massachusetts 02138 USA*
[2]*Department of Physics and Astronomy, University of British Columbia, Vancouver, British Columbia V6T 1Z4 Canada*
[3]*School of Engineering and Applied Sciences, Harvard University, Cambridge, Massachusetts 02138 USA*
[4]*Department of Chemistry and Chemical Biology,*
Harvard University, Cambridge, Massachusetts 02138 USA

We present a new method for nanoscale thermal imaging of insulating thin films using atomic force microscopy (AFM). By sweeping the voltage applied to a conducting AFM tip in contact mode, we measure the local current through a VO$_2$ film. We fit the resultant current-voltage curves to a Poole-Frenkel conduction model to extract the local temperature of the film using fundamental constants and known film properties. As the local voltage is further increased, the nanoscale region of VO$_2$ undergoes an insulator-to-metal transition. Immediately preceding the transition, we find the average electric field to be 32 MV/m, and the average local temperature to be at least 335 K, close to the bulk transition temperature of 341 K, indicating that Joule heating contributes to the transition. Our thermometry technique enables local temperature measurement of any film dominated by the Poole-Frenkel conduction mechanism, and provides the opportunity to extend our technique to materials that display other conduction mechanisms.

Versatile thermal imaging methods are needed to address urgent problems in materials science, semiconductor device technology, and biomedical applications. [1–12] However, few existing methods can accurately map temperatures on the nanoscale. Here, we describe a new scanning probe thermal imaging technique that can operate over a wide range of temperatures, samples, environments, and length scales. To demonstrate the potential of our approach, we perform high spatial resolution temperature mapping to show that local Joule heating can produce an insulator-to-metal transition (IMT) in a voltage-biased VO$_2$ thin film.

Figure 1 characterizes established thermal imaging techniques by their spatial resolution and temperature range. Infrared thermography,[1, 2] Raman spectroscopy,[3] and thermoreflectance[4] are spatially limited by the detected wavelength, and typically do not achieve spatial resolution better than 100 nm.[13] Fluorescence of nanodiamonds[5, 6] or rare earth dopants,[7] Seebeck coefficient thermocouples,[8, 9] thermoresistive probes,[10] and scanning transmission electron microscopy of local plasmon mode[11] techniques have achieved spatial resolutions below 100 nm, however these methods require an initial temperature calibration and measure the relative temperature. Scanning superconducting junctions give excellent absolute sensitivity, but are applicable only in a narrow temperature range.[12]

Here, we demonstrate a new approach to determining the local temperature of an insulating thin film based on the temperature dependence of the Poole-Frenkel[14] (PF) conduction mechanism. We use conductive atomic force microscopy (CAFM) to simultaneously measure a two-dimensional grid of current-voltage (IV) curves and surface topography of a VO$_2$ thin film. From the average film thickness measured by transmission electron
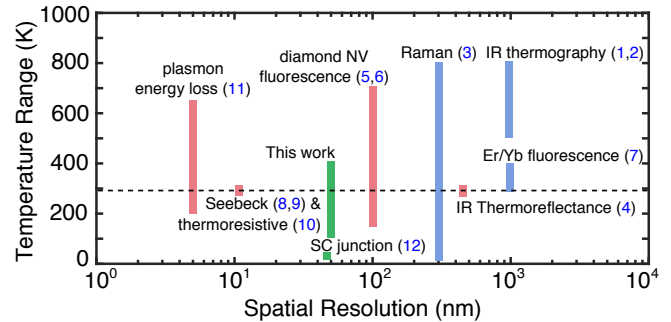

FIG. 1. Demonstrated spatial resolution and temperature range for thermometry techniques. The dotted line is room temperature. Pink bars represent methods that measure the temperature fluctuation about a reference temperature. Blue bars represent models where a calibration is required to measure the temperature over the applicable range. Green bars represent methods where no reference temperature or calibration is required.

microscopy (TEM) (Fig. 2(a)), and the local film thickness variation (Fig. 2(b) and (c)), we determine the film thickness at each point. The IV curves are then fit to the PF mechanism, and by using the known bulk temperature dependence of the film dielectric constant $\varepsilon(T)$, the temperature is the only free parameter.

As a model system we consider VO$_2$, which undergoes a resistivity decrease of up to 5 orders of magnitude as temperature is increased through 341 K.[15] Recently, voltage-triggered switching has also been demonstrated in VO$_2$,[16–22] but the underlying mechanism remains controversial. Previous CAFM studies suggest the importance of Joule heating,[21] while simulations indicate that the current through the insulating state is insufficient to heat most 2-terminal device geometries to the
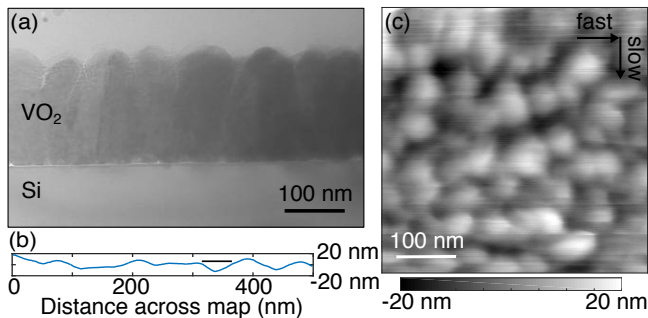
FIG. 2. (a) Cross sectional transmission electron microscopy image of the VO$_2$ film, showing an average thickness of 187 nm. (b) A line cut from the AFM topography, showing the typical variation in film thickness, using the same scale as (a). (c) An AFM image of the surface of the VO$_2$ film, showing individual grains, and varying thickness.
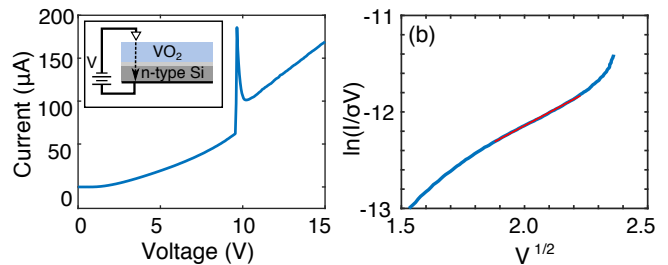

FIG. 3. (a) Typical current vs. voltage (IV) curve, raw data. The sharp increase in current indicates the IMT, but the subsequent spike arises from a stray capacitance in the substrate and external circuit, and is addressed in the Supplementary Information, section 1. Inset: schematic of the data collection geometry. (b) The PF-linearized data shows $\ln(I/\sigma V) \propto V^{1/2}$ immediately preceding the transition. The constant of proportionality, σ has been set to 1 S for the purpose of the plot. The red line is the linear fit used to extract the temperature through the PF model. The contact resistance and external circuit resistance have been removed in (b), leaving only the voltage through the VO$_2$ film.

bulk transition temperature.[23] Here, we use CAFM to acquire a nanoscale map of the lower bound of the local temperature immediately preceding the resistive phase change under applied voltage bias. We find an average film temperature of at least 335 K $\pm$ 4 K, which suggests that in this geometry the IMT is thermally induced by the applied voltage and resultant Joule heating.

The VO$_2$ film was grown by radio frequency sputtering from a VO$_2$ target on a heavily As-doped Si(001) substrate (ρ = 0.002 - 0.005 Ω cm).[21] Room temperature x-ray diffraction measurements[21] are consistent with a polycrystalline, monoclinic VO$_2$ phase. The cross-section TEM image in Fig. 2(a) shows an average film thickness of 187 nm, with a root-mean-square roughness of 6.3 nm, in agreement with the AFM trace in Fig. 2(b). We also use the trace in Fig. 2(b) to estimate the tip contact diameter to be 50 nm, denoted by the bar above the line trace.

We use a home-built AFM with a conductive cantilever in contact mode. All measurements are carried out in high vacuum at room temperature. The cantilever deflection is measured by an interferometer with a wavelength of 1550 nm. A feedback loop controls the z position of the sample to hold the interferometer signal constant, thus maintaining a constant contact force of around 380 nN between the cantilever (spring constant typically k_c = 45 N/m [24]) and sample.[21] Using a contact radius of 25 nm, this corresponds to a pressure of 1.9 kbar, which lowers the transition temperature by 2 K at most.[25] The z position is used to map the local topography in a 500 nm $\times$ 500 nm region as shown in Fig. 2(c). We simultaneously gather local electronic information in this region by sweeping the voltage and measuring the current at each point in a grid pattern with approximately 2 nm separation. We cycle the sample bias from 0 V to 15 V and back, measuring the current at 0.05 V intervals. A typical IV curve is shown in Fig. 3(a). Four consecutive IV sweeps are performed at each point on the map, and are found to

be consistent with each other, ruling out sudden changes in contact resistance or film quality. All data presented here were obtained from the second sweep. This mapping method should be distinguished from previous work on VO$_2$, which presented only individual IV curves at a single location of the sample [21, 22] or current maps acquired by scanning across the sample with a constant sample bias.[21]

At low voltage bias, the VO$_2$ is in an insulating state. As the bias is increased, we observe a sharp jump in current and a subsequent linear relationship between the current and the bias voltage, indicating a transition to the metallic state. Due to a combination of contact resistance and external circuitry, the measured resistance in the metallic state (i.e., the slope of the IV trace) is three orders of magnitude larger than expected for a VO$_2$ thin film alone. Furthermore, the large current transient immediately following the transition arises from a stray series capacitance. As we are interested only in the voltage through the VO$_2$ film in the insulating state, we subtract off the series voltage drop through the substrate and external circuitry (Supplementary Information, section 1).

For each IV curve on the grid, we extract the voltage required to trigger the IMT. The corresponding topographic information is used to compute the electric field at the transition. Figure 4(a) shows a map of the electric field at the IMT, with the corresponding histogram shown in Fig. 4(b). We find the average field across the VO$_2$ film at the IMT is 32 $\pm$ 3 MV/m, consistent with previous reports of an electric field-driven phase transition in VO$_2$.[19, 20, 22] Within each individual VO$_2$ grain there is little variation in electric field at the transition. The grain edges display a higher electric field at transi-

tion, which may be due to local variations in strain or stoichiometry at the boundary,[21] or the AFM tip contacting multiple grains at once.

Having quantified the spread in local electric field at the transition, we return to the central question of the local temperature at the transition. To quantify the local temperature, we investigate the shape of the *IV* curve immediately preceding the transition. We consider several conduction mechanisms in insulators and conclude that PF conduction is the dominant mechanism in this material (Supplementary Information, section 2). PF conduction has previously been observed in VO_2 films, but has not been analyzed to quantify the local temperature.[19, 26]

In an insulating system dominated by PF conduction, the combination of high temperatures and strong electric fields excite trapped electrons into the conduction band,[27] resulting in a current density $\boldsymbol{J}$, given by

$$\boldsymbol{J} = e\mu n|\mathbf{E}| \ \exp\left[\frac{e(e|\boldsymbol{E}|/\pi\varepsilon_0\varepsilon)^{1/2} - e\phi_T}{k_B T}\right]. \quad (1)$$

Here, e is the electron charge, μ is the electron mobility, n is the density of states of the conduction band, $\mathbf{E}$ is the electric field, ε_0 is the permittivity of free space, ε is the relative permittivity of the insulator, ϕ_T is the average trap depth, k_B is the Boltzmann constant, and T is the temperature of the film. Upon rearranging Eqn. 1 for I and V, we obtain

$$\ln\frac{I}{V} = \frac{e^{3/2}}{(\pi\varepsilon_0\varepsilon d)^{1/2} \ k_B T}V^{1/2} + \ln(\sigma) - \frac{e\phi_T}{k_B T}, \quad (2)$$

where $\sigma = ae\mu n/d$ and a is the contact area of the tip, and d is the film thickness. Figure 3(b) shows a PF-linearized *IV* curve, where the red line is the PF slope fit to Eqn. 2.

We fit each PF-linearized *IV* curve, and use the slope $P \equiv e^{3/2}/[(\pi\varepsilon_0\varepsilon d)^{1/2} \ k_B T]$ to calculate the local temperature at each point on the map. Many factors in P are fundamental constants, leaving only the film thickness and relative permittivity to be measured, before determining T. The film thickness is determined in Fig. 2. The relative permittivity has been measured on a separate VO_2/Si(001) film, in an experiment where the global temperature of the film was varied from 290 K to 333 K (Supplementary Information, section 3). The interpolated function $\varepsilon(T)$ is then used to self-consistently determine the temperature associated with each *IV* curve on our map. The calculated temperature map and corresponding histogram are shown in Figs. 4(c) and 4(d). Similar to the map of the electric field at the IMT, individual grains are discernible due to abrupt changes at grain boundaries.

Our analysis indicates an average temperature of 335 K prior to the IMT over the region of interest, with a standard deviation of 4 K. Additionally, we calculate

an uncertainty of 4 K for each individual temperature measurement from uncertainties in d, $\varepsilon(T)$, and fitted slope (Supplementary Information, section 4). The average temperature is well above room temperature and just below the known bulk transition temperature of 341 K,[15, 16] which suggests Joule heating has locally caused the sample to heat close to its transition temperature. The sharp cut-off in our measured transition temperatures at 341 K supports the validity of our technique. We note that the finite voltage range required for fitting means that the extracted temperature is an average over an interval immediately preceding the transition; the instantaneous temperature at the end of this interval is presumably even larger and closer to the bulk transition temperature.

We have invented a new nanoscale thermal imaging technique to address the long debate of whether or not the electronic phase transition in VO_2 can be triggered by an applied electric field.[19, 20, 22] However, this technique may also be applied to other materials that display PF conduction, including Pr_2O_3[28], and simple binary oxides such as ZnO[29], SnO_x, AlO_x, CeO_x and WO_x,[30] which have attracted attention as an alternative gate dielectric,[31] and for resistive switching devices.[29]

Our approach can be extended to insulating materials dominated by other conduction mechanisms, such as Schottky field emission, Fowler-Nordheim tunneling, thermionic-field emission, hopping conduction, Ohmic conduction, and ionic conduction[27]. Each of these mechanisms can be linearized in terms of current and voltage, with a slope that is dependent on the film temperature and various parameters, depending on the mechanism. These parameters include a combination of fundamental constants and film-dependent properties. For example, in hopping conduction the linearized slope depends on fundamental constants, film thickness, and the hopping distance between traps. In order to accurately measure the temperature with the hopping conduction mechanism, the hopping distance would have to be known or assumed to produce reliable results. The CAFM thermometry technique could therefore be extended to any film dominated by one of these conduction mechanisms once the film-dependent parameters are known. However, the PF conduction mechanism is most conducive to accurate thermometry, since there are no unknown free parameters.

In conclusion, we used a new CAFM-based technique to measure the local temperature of a VO_2 thin film. We find that Joule heating increases the temperature of the film to around 335 K, which indicates that the IMT is not solely triggered by the applied electric field in our geometry. This technique is capable of measuring the local temperature of a film with a spatial resolution limited only by the contact area of the tip (radius $\lesssim$ 25 nm in our experiment, but potentially as small as 10 nm [32]) and a temperature uncertainty of 4 K, without the use
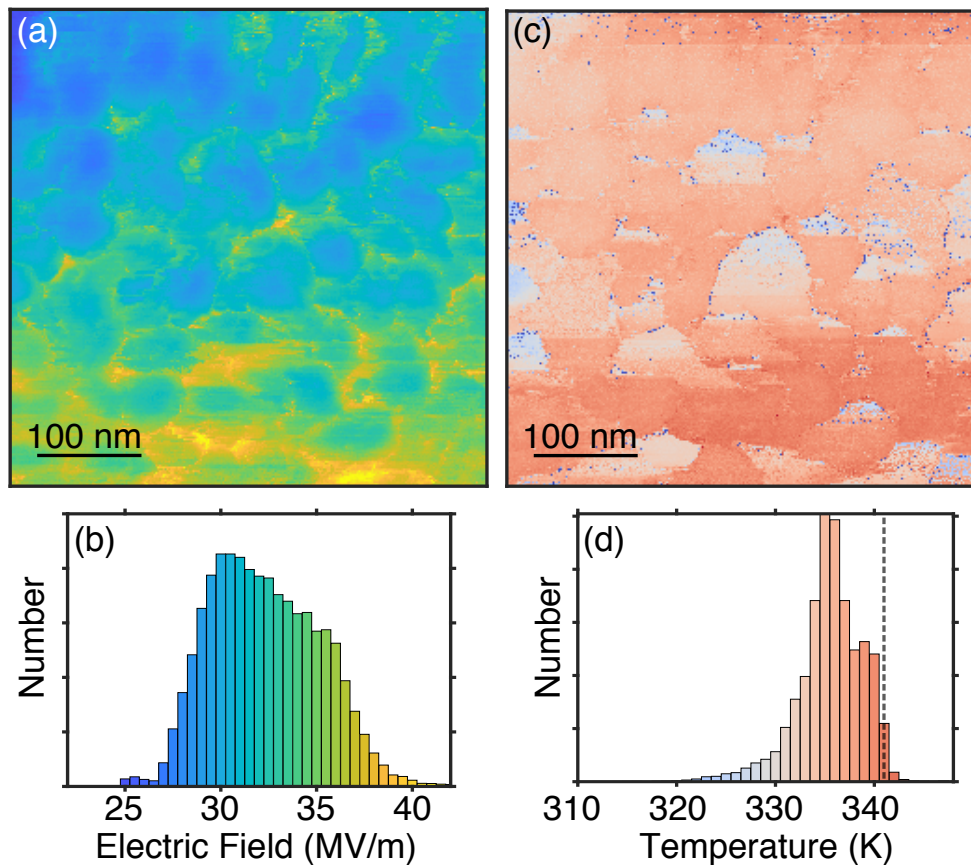
FIG. 4. (a) Map of the electric field required to trigger the IMT. (b) Histogram of the map from (a). (c) Map of the local temperature preceding the transition. All maps are from the same region of the sample as shown in Fig. 1(c). (d) Histogram of the temperature map in (c). The dotted line denotes the IMT transition temperature of the film. We note the sharp drop for values greater than the IMT temperature of 341 K.

of a reference temperature or unknown free parameters. The use of IV curves acquired through CAFM as a local temperature probe may be applied to a wide range of insulating thin films systems to address questions in materials science and novel nanoscale devices.

* jhoffman@physics.harvard.edu
† jasonhoffman@fas.harvard.edu

[1] D. Teyssieux, L. Thiery, and B. Cretin, "Near-infrared thermography using a charge-coupled device camera: Application to microsystems," Review of Scientific Instruments **78**, 034902 (2007).

[2] J. S. Lee, M. Ortolani, U. Schade, Y. J. Chang, and T. W. Noh, "Time-resolved visualization of the heat flow in VO_2/Al_2O_3 films," Applied Physics Letters **90**, 051907 (2007).

[3] J. S. Reparaz, E. Chavez-Angel, M. R. Wagner, B. Graczykowski, J. Gomis-Bresco, F. Alzina, and C. M. Sotomayor Torres, "A novel contactless technique for thermal field mapping and thermal conductivity determination: Two-laser Raman thermometry," Review of Scientific Instruments **85**, 034901 (2014).

[4] G. Tessier, M. Bardoux, C. Boué, C. Filloy, and D. Fournier, "Back side thermal imaging of integrated circuits at high spatial resolution," Applied Physics Letters **90**, 171112 (2007).

[5] G. Kucsko, P. C. Maurer, N. Y. Yao, M. Kubo, H. J. Noh, P. K. Lo, H. Park, and M. D. Lukin, "Nanometre-scale thermometry in a living cell," Nature **500**, 54–58 (2013).

[6] P. Neumann, I. Jakobi, F. Dolde, C. Burk, R. Reuter, G. Waldherr, J. Honert, T. Wolf, A. Brunner, J. H. Shim, D. Suter, H. Sumiya, J. Isoya, and J. Wrachtrup, "High-precision nanoscale temperature sensing using single defects in diamond," Nano Letters **13**, 2738–2742 (2013).

[7] Lionel Aigouy, Gilles Tessier, Michel Mortier, and Benoît Charlot, "Scanning thermal imaging of microelectronic

circuits with a fluorescent nanoprobe," Applied Physics Letters **87**, 184105 (2005).

[8] Seid Sadat, Aaron Tan, Yi Jie Chua, and Pramod Reddy, "Nanoscale thermometry using point contact thermocouples," Nano Letters **10**, 2613–2617 (2010).

[9] Kyeongtae Kim, Wonho Jeong, Woochul Lee, and Pramod Reddy, "Ultra-high vacuum scanning thermal microscopy for nanometer resolution quantitative thermometry," ACS Nano **6**, 4248–4257 (2012).

[10] Fabian Menges, Philipp Mensch, Heinz Schmid, Heike Riel, Andreas Stemmer, and Bernd Gotsmann, "Temperature mapping of operating nanoscale devices by scanning probe thermometry," Nature Communications **7**, 10874 (2016).

[11] Matthew Mecklenburg, William A. Hubbard, E. R. White, Rohan Dhall, Stephen B. Cronin, Shaul Aloni, and B. C. Regan, "Nanoscale temperature mapping in operating microelectronic devices," Science **347**, 629–633 (2015).

[12] D. Halbertal, J. Cuppens, M. Ben Shalom, L. Embon, N. Shadmi, Y. Anahory, H. R. Naren, J. Sarkar, A. Uri, Y. Ronen, Y. Myasoedov, L. S. Levitov, E. Joselevich, A. K. Geim, and E. Zeldov, "Nanoscale thermal imaging of dissipation in quantum systems," Nature **539**, 407–410 (2016).

[13] Carlos D. S. Brites, Patricia P. Lima, Nuno J. O. Silva, Angel Millan, Vitor S. Amaral, Fernando Palacio, and Luis D. Carlos, "Thermometry at the nanoscale," Nanoscale **4**, 4799– 4829 (2012).

[14] J. Frenkel, "On pre-breakdown phenomena in insulators and electronic semiconductors," Physical Review **54**, 647–648 (1938).

[15] F. J. Morin, "Oxides which show a metal-to-insulator transition at the Neel temperature," Physical Review Letters **3**, 34–36 (1959).

[16] M. M. Qazilbash, Z. Q. Li, V. Podzorov, M. Brehm, F. Keilmann, B. G. Chae, H. T. Kim, and D. N. Basov, "Electrostatic modification of infrared response in gated structures based on VO_2," Applied Physics Letters **92**, 241906 (2008).

[17] G. Stefanovich, A. Pergament, and D. Stefanovich, "Electrical switching and mott transition in VO_2," Journal of Physics: Condensed Matter **12**, 8837–8845 (2000).

[18] Hyun-Tak Kim, Byung-Gyu Chae, Doo-Hyeb Youn, Sung-Lyul Maeng, Gyungock Kim, and Kwang-Yong Kang, "Mechanism and observation of mott transition in VO_2-based two- and three-terminal devices," New Journal of Physics **6**, 52 (2004).

[19] Changhyun Ko and Shriram Ramanathan, "Observation of electric field-assisted phase transition in thin film vanadium oxide in a metal-oxide-semiconductor device geometry," Applied Physics Letters **93**, 252101 (2008).

[20] Dmitry Ruzmetov, Gokul Gopalakrishnan, Jiangdong Deng, Venkatesh Narayanamurti, and Shriram Ramanathan, "Electrical triggering of metal-insulator transition in nanoscale vanadium oxide junctions," Journal of Applied Physics **106**, 083702 (2009).

[21] Jeehoon Kim, Changhyun Ko, Alex Frenzel, Shriram Ramanathan, and Jennifer E. Hoffman, "Nanoscale imaging and control of resistance switching in VO_2 at room temperature," Applied Physics Letters **96**, 213106 (2010).

[22] B. Wu, A. Zimmers, H. Aubin, Y. Ghosh, R .and Liu, and R. Lopez, "Electric-field-driven phase transition in vanadium dioxide," Physical Review B **84**, 241410 (2011).

[23] Gokul Gopalakrishnan, Dmitry Ruzmetov, and Shriram Ramanathan, "On the triggering mechanism for the metal – insulator transition in thin film VO_2 devices : electric field versus thermal effects," Journal of Materials Science **44**, 5345–5353 (2009).

[24] "Cantilever purchased from μmasch: https://www.spmtips.com/afm-tip-hq-nsc16-cr-au,".

[25] Larry A. Ladd and William Paul, "Optical and Transport Properties of High Quality Crystals of V_2O_4 Near the Metallic Transition temperature," Solid State Communications **7**, 425–428 (1969).

[26] Zheng Yang, Changhyun Ko, Viswanath Balakrishnan, Gokul Gopalakrishnan, and Shriram Ramanathan, "Dielectric and carrier transport properties of vanadium dioxide thin films across the phase transition utilizing gated capacitor devices," Physical Review B **82**, 205101 (2010).

[27] Fu-Chien Chiu, "A review on conduction mechanisms in dielectric films," Advances in Materials Science and Engineering **2014**, 578168 (2014).

[28] Fu-Chien Chiu, Chun-Yen Lee, and Tung-Ming Pan, "Current conduction mechanisms in Pr_2O_3/oxynitride laminated gate dielectrics," Journal of Applied Physics **105**, 074103 (2009).

[29] Wen-Yuan Chang, Yen-Chao Lai, Tai-Bor Wu, Sea-Fue Wang, Frederick Chen, and Ming-Jinn Tsai, "Unipolar resistive switching characteristics of ZnO thin films for nonvolatile memory applications," Applied Physics Letters **92**, 022110 (2008).

[30] Ee Wah Lim and Razali Ismail, "Conduction mechanism of valence change resistive switching memory: A survey," Electronics **4**, 586–613 (2015).

[31] By Raffaella, Lo Nigro, Roberta G Toro, Graziella Malandrino, Vito Raineri, and Ignazio L Fragalà, "A simple route to the synthesis of Pr_2O_3 high-k thin films," Advances in Materials Science and Engineering **15**, 1071–1075 (2003).

[32] Jason H. Hafner, Chin Li Cheung, and Charles M. Lieber, "Growth of nanotubes for probe microscopy tips," Nature **398**, 761–762 (1999).